Apoptosis (2011) 16:1195–1204
DOI 10.1007/s10495-011-0647-4

ORIGINAL PAPER

Fas/FasL pathway-mediated alveolar macrophage apoptosis involved in human silicosis

San-qiao Yao · Liying Wang Rojanasakul · Zhi-yuan Chen · Ying-jun Xu · Yu-ping Bai · Gang Chen · Xi-ying Zhang · Chun-min Zhang · Yan-qin Yu · Fu-hai Shen · Ju-xiang Yuan · Jie Chen · Qin-cheng He

Published online: 11 September 2011

Abstract In vitro and in vivo studies have demonstrated that lung cell apoptosis is associated with lung fibrosis; however the relationship between apoptosis of alveolar macrophages (AMs) and human silicosis has not been addressed. In the present study, AM apoptosis was determined in whole-lung lavage fluid from 48 male silicosis patients, 13 male observers, and 13 male healthy volunteers. The relationships between apoptosis index (AI) and silica exposure history, soluble Fas (sFas)/membrane-bound Fas (mFas), and caspase-3/caspase-8 were analyzed. AI, mFas, and caspase-3 were significantly higher in lung lavage fluids from silicosis patients than those of observers or healthy volunteers, but the level of sFas demonstrated a decreasing trend. AI was related to silica exposure, upregulation of mFas, and activation of caspase-3 and -8, as well as influenced by smoking status after adjusting for confounding factors. These results indicate that AM apoptosis could be used as a potential biomarker for human silicosis, and the Fas/FasL pathway may regulate this process. The present data from human lung lavage samples may help to understand the mechanism of silicosis and in turn lead to strategies for preventing or treating this disease.

Keywords Silicosis · Alveolar macrophages · Apoptosis · Soluble Fas · Membrane-bound Fas · Caspase

S. Yao · J. Chen · Q. He (✉)
Division of Pneumoconiosis, School of Public Health, China Medical University, 92 North 2nd Road, Heping District, Shenyang 110001, China
e-mail: qche@mail.cmu.edu.cn

S. Yao
e-mail: sanqiaoyao@qq.com

J. Chen
e-mail: chenjie@mail.cmu.edu.cn

S. Yao · Y. Xu · Y. Bai · X. Zhang · C. Zhang · Y. Yu · F. Shen · J. Yuan
Department of Occupational and Environmental Health, School of Public Health, Hebei United University, 57 Jianshe South Avenue, Lubei District, Tangshan, Hebei 063000, China
e-mail: xyj5308@yahoo.com.cn

Y. Bai
e-mail: yp631121@yahoo.com.cn

X. Zhang
e-mail: zxy7408@yahoo.com.cn

C. Zhang
e-mail: chunmin2006@sina.com

Y. Yu
e-mail: yuyanqin1@sina.com

F. Shen
e-mail: shfh600@163.com

J. Yuan
e-mail: yuanjx@heuu.edu.cn

S. Yao · Y. Xu · Y. Bai · C. Zhang · F. Shen · J. Yuan
Key Lab for Coal Mine Health and Safety of Hebei Province, 57 Jianshe South Avenue, Lubei District, Tangshan, Hebei 063000, China

L. W. Rojanasakul
Pathology and Physiology Research Branch, National Institute for Occupational Safety and Health (NIOSH), 1095 Willowdale Road, Morgantown, WV 26505, USA
e-mail: lmw6@cdc.gov

Z. Chen · G. Chen
Department of Pneumoconiosis, Beidaihe Sanitarium for China Coal Miners, Bao 2nd Road, Seashore Beidai, Hebei 066104, China
e-mail: czyuan@heinfo.net

G. Chen
e-mail: cg710121@126.com

Introduction

Silicosis is a chronic lung disease characterized by granulomatous and fibrotic lesions due to the accumulation of inhaled silica particles. Chronic human silicosis results primarily from continued occupational exposure to silica and demonstrates a long asymptomatic latency. Intratracheal exposure to large doses of silica can induce acute silicosis characterized by granuloma-like formations in the lung associated with apoptosis, severe alveolitis, and alveolar lipoproteinosis [1]. Alveolar macrophage (AM) apoptosis itself is an important event in silicosis and has been associated with innate immune cell infiltration and increased collagen deposition [2].

AMs have been suggested to play crucial roles in the initiation and progression of lung silicosis. AM activation upon exposure to silica particles in the lungs has been well documented and results in the release of macrophage products including fibrogenic factors, lysosomal enzymes, free radicals, and cytokines [3]. Studies have indicated that silica also has the ability to induce apoptosis in AMs, but relatively little is known regarding the underlying mechanisms involved [4]. Silica particles induce lung cell apoptosis through specific molecular mechanisms that may be mediated by factor-related apoptosis (Fas)/Fas ligand (FasL) interactions [5], an apoptosis pathway. Although much is known about the apoptotic machinery following silica exposure in rodent models, data from humans is still lacking.

The limited information concerning the relationship between human AM apoptosis and silicosis is due to the difficulty in obtaining human lung cells. Currently, the use of massive whole-lung lavage as part of the treatment for silicosis patients in China allows us to collect human AMs and analyze AM apoptosis. Determining how silica induces Fas and caspase activation along with AM apoptosis in silicosis will provide insight on potential factors that may be used as biomarkers for early silicosis diagnosis. Furthermore, understanding the relationship between silica exposure and AM apoptosis will also provide clues to understanding the pathogenesis and mechanism of human silicosis, which are urgently needed for silicosis prevention and treatment.

Materials and methods

Subjects

Sixty-one male silica-exposed workers who were diagnosed as observers whose X-ray photographs had uncertain silicosis-like changes, the nature and severity not dynamically changed within 5 years, and silicosis patients (at stages I, II III) as determined by X-ray photograph were included in the study. All subjects were of Han nationality and from all over China. Silicosis was diagnosed by a local pneumoconiosis diagnosis group according to the standard of GBZ70-2009 issued in China and ILO-2000. Thirteen healthy male volunteers were selected as a control group, who were of Han nationality and from the same living area and age group as observers and silicosis patients but never exposed to silica dust. None of these subjects presented clinical signs/symptoms of autoimmune diseases including sclerotic skin, Raynaud's phenomenon, facial erythema, arthralgia, and malignancies. The backgrounds of the subjects, including sex, age, nationality, and career history, were collected by questionnaires. They all underwent massive whole-lung lavage at the "Beidaihe Sanatorium for China Coal Miners" from January to December 2009. All subjects signed informed consent forms before the lavage. The project was approved by the Medical Ethics Committee of China Medical University.

Reagents and antibodies

Dulbecco's modified eagle medium (DMEM) was purchased from Santa Cruz Biotechnology Inc. (Santa Cruz, CA, USA). Sodium-dodecyl sulfate (SDS) was purchased from Sigma-Aldrich Co. (St. Louis, MO, USA). Acrylamide, *N*′*N*-methylenebisacrylamide, and ammonium persulfate were purchased from Biomol International (Plymouth Meeting, PA, USA). Tetramethylethylenediamine was purchased from Ameresco Inc. (Framingham, MA, US). Antibodies (Abs) directed against human Fas, caspase-8, caspase-3, and β-actin were purchased from Santa Cruz Biotechnology Inc. (Santa Cruz, CA, USA). Hoechst 33258 and fluorescein isothiocyanate (FITC)-conjugated anti-human CD68 were purchased from eBioscience Inc. (San Diego, CA, USA). Human Fas, Caspase-8 and -3 ELISA assay kit were purchased from R&D Systems (Minneapolis, MN, USA). BCA protein assay kit was purchased from Thermol Scientific Company (Portsmouth, NH, USA). Other chemicals and reagents were purchased from Wastson Biotech Company LTD (Tianjin, China).

AM isolation, purification and culture

The lavage fluids of all subjects were collected into aseptic containers, filtered through double-layer gauze to remove mucus, centrifuged at 1500 rpm, and washed 3 times with PBS buffer. Cells were counted using a hemocytometer after being separated from lavage fluid. After the cells were counted, AMs were purified in DMEM containing 10% fetal calf serum under 5% CO_2 at 37°C for 2 h based on their adherence. The purification rate of AMs was 95–99%, confirmed by staining with 10 μg/ml FITC anti-human CD68 for 30 min. After nonadherent non-AM cells were

washed, the adherent purified AMs were incubated at 37°C for another 24 h and harvested. The harvested AMs and supernatant liquids were stored at −80°C until use in the studies below.

Apoptosis detection under light microscope

After purified AMs from 5 volunteers, 5 observers, and 15 silicosis patients (5 stage-I, II, III, respectively) were harvested, an AM suspension (0.1 ml) containing 1×10^6 purified AMs/ml was smeared onto a glass slide and fixed with 4% paraformaldehyde for 1 h. The slides were washed with PBS, stained with 0.5% hematoxylin for 10 min, and washed with water. They were then differentiated with hydrochloric acid-alcohol and stained with 0.5% eosin for 3 min. Morphological characteristics were observed under a light microscope.

Apoptosis detection under transmission electron microscope (TEM)

Purified AMs (1×10^6 AMs/sample) from 15 subjects including healthy volunteers, observers, and silicosis patients at stage I, II, and III were fixed with 2.5% glutaraldehyde, postfixed for 1 h in 1% osmium tetroxide, dehydrated in acetone, and embedded in Epon 812. Thin sections were stained with uranyl acetate/lead citrate and observed under a Hitachi H-7650 transmission electron microscope operated at 80 kV. Images of each sample were collected from six visual fields.

Apoptosis detection with flow cytometry (FCM) analysis

Purified AMs (5×10^6) from all subjects were washed with PBS and fixed with 70% cold alcohol at 4°C for at least 12 h. After centrifugation and washing with PBS, fixed AMs were incubated with RNase for 30 min at 37°C, then treated with propidium iodide in the dark at 4°C for 30 min. Treated AMs in suspension (0.5 ml, corresponding to at least 1×10^6 cells) were infiltrated with 50-μm nylon net. FCM was performed with a Coulter EPICS XL cytometer with a gate set for examining a total of 10^4 AMs. Apoptosis index (AI), the percentage of apoptotic AMs among total AMs was calculated to within 10^4 AMs.

Apoptosis detection under laser scanning confocal microscope (LSCM)

AMs from 5 volunteers, 5 observers, 15 silicosis patients(5 stage-I, II, III, respectively) (5×10^6 AMs/subject) were suspended in binding buffer with 10 μg/ml Hoechst 33258 and 10 μg/ml FITC anti-human CD68 and rocked gently in the dark. AMs were centrifuged and smeared onto a glass slide with fluorescent free glycerin. AM nuclei were stained blue, and the membranes were stained green. The morphological characteristics of AM nuclei were observed immediately under a FV-1000 Olympus LSCM using FV10-ASW software. Images of each sample were collected from six visual fields.

DNA fragmentation analysis

Purified AMs from 5 volunteers, 5 observers, and 5 stage-I silicosis patients (5×10^6 AMs/subject) were harvested, by the high salt method [6] to extract genome of AMs. Each DNA solution was applied to a 11 × 14 horizontal agarose (1.5%) gel pre-stained with 5 μg/ml ethidium bromide and separated by electrophoresis. The gel was placed into a UVI GEL imaging system purchased from BD Company (Franklin Lakes, NJ USA) and photographed under ultraviolet light. AMs from one volunteer were treated with 0.5 mM H_2O_2 for 12 h to be used as positive control for the DNA fragmentation analysis as mentioned above.

ELISA assay

The total protein concentration of all subjects was measured with the BCA protein assay kit. The levels of soluble Fas (sFas) in supernatants from all subjects were detected with a human Fas ELISA kit. Blanks, standards, and samples were added separately to 96-well plates. Each sample was analyzed in triplicate. After mixing by gentle shaking, plates were incubated for 30 min at 37°C, washed 5 times, and 50 μl HRP-conjugate reagent was added to each well. After incubation for 30 min at 37°C and washing, chromogen solutions A (50 μl) and B (50 μl) were added and incubated for 10 min. Stop solution (50 μl) was then added to each well to stop the reaction. The blank well was set as zero, and the optical density (OD) of each well at 450 nm was measured within 15 min.

Western blotting

Protein was extracted from the AMs of all subjects by using western blot protocol recommended by Milipore [7]. Total protein extracts were loaded on a 10% polyacrylamide gel (30 μg/well) and electrophoretically transferred to nitrocellulose (NC) filters. After blocking for 2 h with 5% nonfat milk buffer in TBST, the membranes were incubated overnight at 4°C with rabbit anti-human Fas, mouse anti-human caspase-8, mouse anti-human caspase-3, or mouse anti-human β-actin Abs diluted 1:2000 in 5% nonfat milk-TBST. The NC filters were washed and incubated for 1 h with peroxidase-conjugated IgG diluted 1:4000. The protein bands were visualized using the ECL

system (Pierce, Miami, FL) and analyzed by densitometry using Microtek Scan Wizard 5 scan software and Quantity One 7.0 imaging analysis software. Membrane-bound Fas (mFas), caspase-8, and -3 were quantified by the gray-scale value of mFas, caspase-8 and -3 adjusted by the gray-scale value of each subject' β-actin.

Statistics

The data was managed using Excel software. STATA 10.0 software was used to analyze differences in AM apoptosis, sFas, mFas, caspase-8, and -3 between various silicosis-associated factors as well as the relationship between Fas, caspase-8, -3, and apoptosis. The Poisson generalized linear regression model was used to analyze the factors related to AM apoptosis.

Results

Basic information about subjects

The mean age of 61 silica-exposed workers was 46.27 ± 7.69 (32–59) year, and the mean duration from silica exposure to lung lavage was 16.9 ± 11.1 (1–37) year. The mean duration from cessation of silica exposure to lung lavage was 5.9 ± 7.8 (0–30) year, and the smoking rate was 65.6%. The information for all subjects is presented in Table 1. No statistically significant difference in age and smoking rate was observed between healthy volunteers, observers, and silicosis patients. No difference in the duration from silica exposure to lung lavage and duration of cessation of silica exposure was found among silicosis groups.

The morphological characteristics of apoptotic AMs under light microscope, TEM, and LSCM

TEM imaging is considered the gold standard in identifying cellular apoptosis because of its standard and reliable method. Typical apoptotic morphological changes were observed in AM from silicosis patients, which were confirmed under LSCM and FCM. Figure 1 shows apoptotic AMs under a light microscope, TEM, LSCM, and FCM. Normal AMs demonstrated a smooth membrane and homogeneous chromatin (Fig. 1A a), while apoptotic AMs appeared to shrink and presented other characteristics including membrane blebbing, chromatin condensation (Fig. 1A b), nuclear membrane disintegration, smashed nucleus and apoptotic body formation with dust particles in the cytoplasm (Fig. 1A c), and a crescent formation (Fig. 1A d).It also was observed that the severity of apoptotic AMs increased with the progression of silicosis (Fig. 1A d–h).

Under LSCM, AM nuclei were stained blue by Hoechst 33258 (Fig. 1B a, b), and membranes were stained green by FITC-conjugated anti-human CD68 (Fig. 1B a, b). The nuclei of normal AMs were round or ellipse, with chromatin uniformity and integrated nuclear membrane

Fig. 1 Apoptotic AMs visualized using a light microscope, TEM, LSCM and FCM. **A** AMs apoptosis analysis by light microscope (H&E stain, 1000×). (*a*) normal AMs from volunteers; (*b*) apoptotic AMs from silicosis patient at stage I showed the shrinkage phenotype; (*c*) AMs from silicosis patient at stage II showed crescent; (*d*) AM apoptotic bodies from silicosis patient at stage III; Again, *e–h* showed clear AM morphology from normal (*e*), observer (*f*), silicosis stage 1 (*g*) and silicosis stage III (h). **B** AMs apoptosis by LSCM (Hoechst 33258, FITC anti-human CD68) (400×), (*a*) normal AMs from volunteer; (*b*) apoptotic AMs from silicosis patient at stage I. The AMs were also checked for AM cell purity with FITC anti-human CD68. It showed that the AM purify rate was 99% under FCM (*c*). (*d*) AMs with some apoptotic nuclear from volunteer; (*e*) AMs with marginalization chromatin from observer; (*f*) AMs with condensational chromatin from silicosis at stage II; (*g*) AMs with breakage nuclear from silicosis at stage III. **C** Apoptotic AMs under TEM analysis. (*a*) normal AMs from volunteer (7000×); (*b*) AMs from observer with chromatin marginalization (*yellow arrow*); (*c*) AMs from silicosis at stage I compared to AMs from silicosis at stage II (*d*) with nuclear breakage (*red arrow*) and crescent formation (*black arrow*) (5000×); (*e*) AMs from silicosis at stage I compared to AM from stage II silicosis with chromatin condensation (*f*, *black arrow*, 10000×); AM apoptosis from stage III patients showed typical apoptotic bodies (*g*), mitochondrial swelling (*h*) and lysosome autophagy (*i*)

Table 1 Subjects' basic information

Group	n	Age (year)	Duration of silicon exposure (year)	Smoking (%)	Duration of cessation of silicon exposure (year)
Health volunteers	13	45.6 ± 9.1	ND	7 (53.8)	ND
Observers	13	45.2 ± 8.2	14.2 ± 10.4	8 (61.5)	7.3 ± 9.7
Silicosis at stage I	33	48.1 ± 7.3	18.7 ± 11.7	21 (63.6)	5.8 ± 7.6
Silicosis at stage II	11	45.2 ± 7.5	18.1 ± 9.8	9 (81.8)	5.5 ± 6.7
Silicosis at stage III	4	38.0 ± 3.8	6.5 ± 5.2	2 (50.0)	3.5 ± 5.7
Silica-exposed workers[a]	61	46.3 ± 7.7	16.9 ± 11.1	40 (65.6)	5.9 ± 7.8
F/χ^2		2.46	1.84	1.86	0.397
P		0.072	0.151	0.601	0. 941

[a] Indicates observers and all silicosis patients

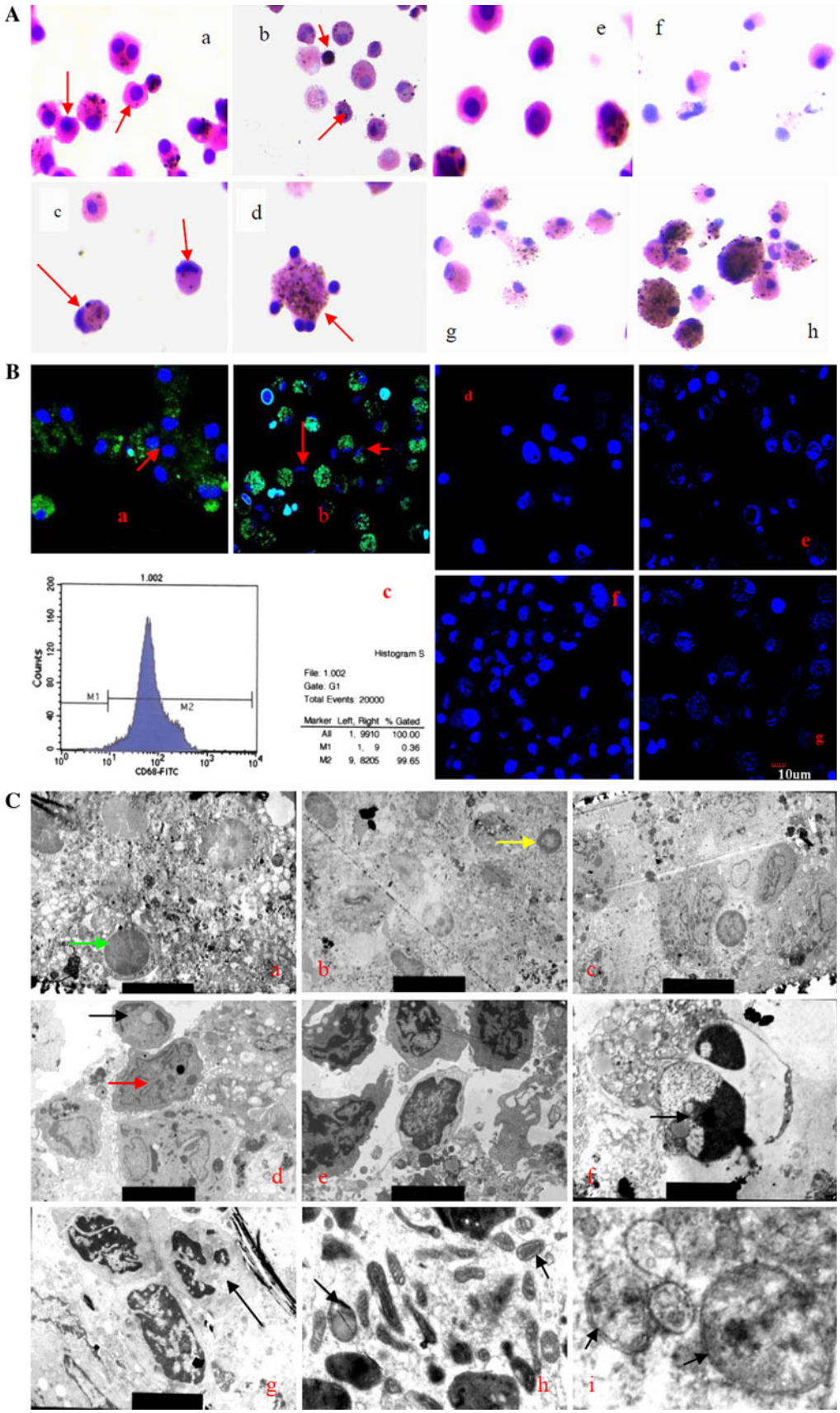
A
a
b
e
f
c
d
g
h
B
a
b
d
e
c
f
g
10um
1.002
Counts
M1
M2
CD68-FITC
Histogram S
File: 1.002
Gate: G1
Total Events: 20000
Marker Left, Right % Gated
All 1, 9910 100.00
M1 1, 9 0.36
M2 9, 8205 99.65
C
a
b
c
d
e
f
g
h
i

(Fig. 1B a, red arrow). The nuclear morphology of apoptotic AMs included ripples or creases, chromatin condensation, marginalization, breakage, and apoptotic body formation (Fig. 1B b). The nuclear damage was increased with the progression of silicosis (Fig. 1B d–g).

TEM analysis indicated that the number of apoptotic AMs and chromatin change increased with the progression of silicosis (Fig. 1C a–e). Apoptotic AMs demonstrated chromatin marginalization (Fig. 1C b, yellow arrow), nuclear breakage (red arrow), crescent formation (black arrow) (Fig. 1C d), chromatin condensation (Fig. 1C f, black arrow), and apoptotic body formation (Fig. 1C g, black arrow). Additionally, an increased number of mitochondria and endoplasmic reticulum, mitochondrial swelling (Fig. 1C h, black arrow), and autophagy (Fig. 1C i, black arrow) were also observed under TEM.

DNA fragmentation, apoptosis by scatter diagram and histogram, and Fas, Caspase-8 and -3 expression

Elevated $Ca^{2+}$and Mg^{2+} can activate intracellular endonucleases when cells undergo apoptosis. The activated endonuclease can lead to double-chain DNA breakage, with fragments of 180–200 bp or integral multiples. The DNA fragmentation leads to "ladder" formation in agarose gel electrophoresis. The present study demonstrated typical DNA ladder formation in patient AMs. The molecular weight of genomic DNA from stage-I silicosis patient AMs and a positive control sample was approximately 180 bp or its integral multiple (Fig. 2A). No bands were observed in genomic DNA collected from observer AMs.

The Fas signaling pathway is thought to play a crucial role in silica particle-induced apoptosis. It is typically

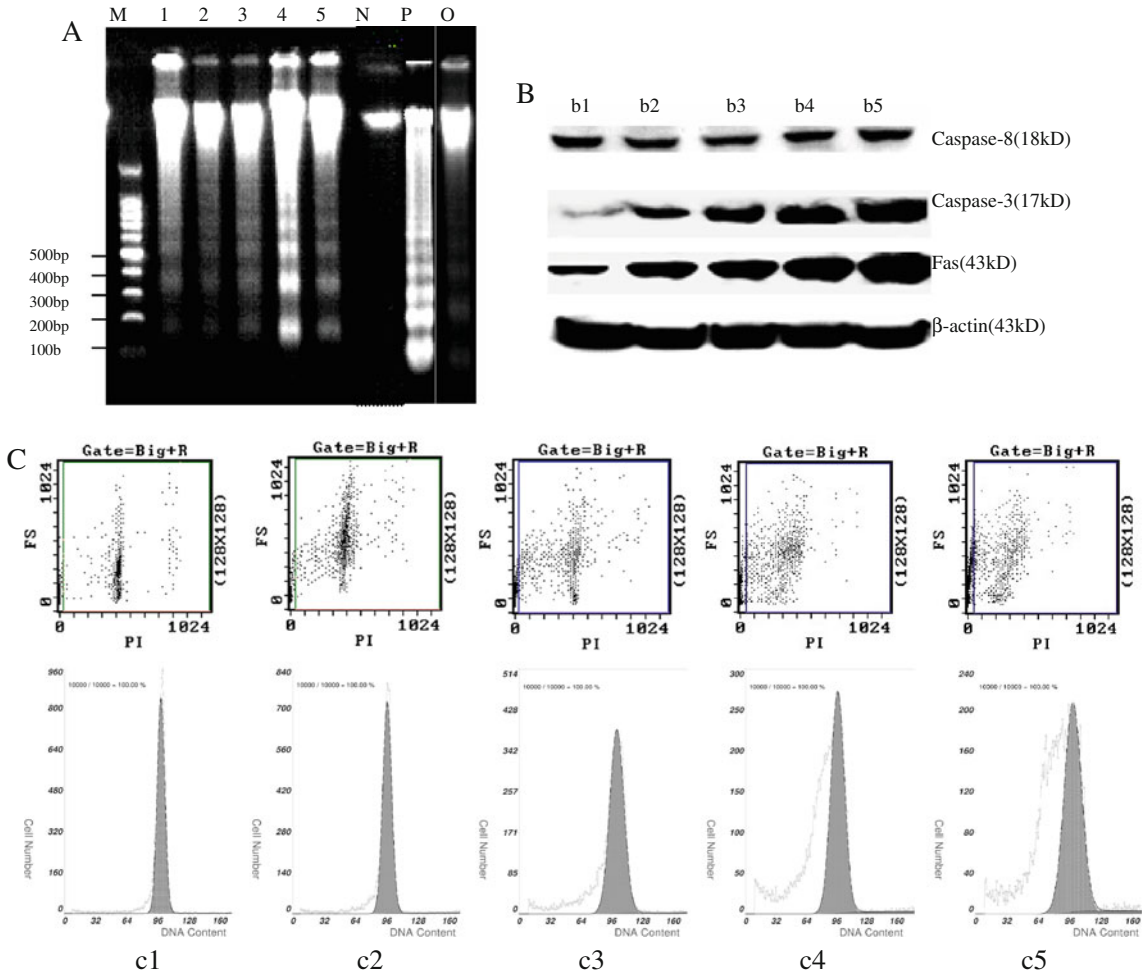

Fig. 2 Molecular biology and histogram analysis of AM apoptosis from silicosis patients compared to controls. **A** DNA fragmentation, *M* Marker, *1–5* five silicosis patients at stage I, *N* health volunteer, *P* positive control, *O* observer. **B** Expression of mFas, Caspase-8, -3 of subjects, *b1* health volunteer, *b2* observer, *b3* silicosis at stage I, *b4* silicosis at stage II, *b5* silicosis at stage III. **C** Scatter diagram and histogram of apoptotic AMs by FCM, *c1* health volunteer, *c2* observer, *c3* silicosis at stage I, *c4* silicosis at stage II, *c5* silicosis at stage III

mediated through caspase activation, with an effector caspase (e.g., caspase-3) activated by a coordinated hierarchy of initiator caspases (e.g., caspases-8). As shown in Fig. 2B, the relative quantities of mFas and Caspase-3 increased with the progression of silicosis (Fig. 2B, B1 and B2) but the change of caspase-8 was not obvious. FCM has the advantage of detecting apoptosis both in quality and quantity. The fluorescent intensity is proportional to the quantity of DNA. In this study, we found that the degree of AM apoptosis of silicosis patients was higher than those of healthy volunteers and observers based on scatter diagram and histogram (Fig. 2C).

The relationship between Fas, caspases, AI, and factors related to silicosis

To explore the relationship between silicosis and AM apoptosis, Fas, and caspase expression, apoptotic AM number and sFas level were measured in supernatant of cultured AMs from lung lavage fluids of various patients, and mFas, caspase-8, and -3 expression was quantified in AMs. The results are shown in Table 2. The AI of silica-exposed workers was higher than that of healthy volunteers and increased with the progression of silicosis, but no significant difference was noted between healthy volunteers and observers. mFas and caspase-3 were found to increase with the progression of silicosis, but sFas demonstrated the opposing trend. Caspase-8 did not significantly differ among groups.

The relationship between AM apoptosis, Fas level, caspase-3 expression, and silica exposure

To determine the role of AM apoptosis in the development and progression of silicosis, the relationship between the AI of AMs and factors including age, age at first silica exposure, duration from silica exposure to lung lavage, age of patients at the onset of pneumoconiosis, duration from silica exposure to silicosis onset, duration from cessation of silica exposure to lung lavage, and silicosis type was analyzed. Smoking was also considered as a main confounding factor.

As shown in Table 3, longer duration from silica exposure to lung lavage and shorter duration from silica exposure to silicosis onset were associated with higher AI, mFas, and caspase-3 and lower caspase-8 in silicosis patients. The mFas level was lower and sFas level was higher in patients with cessation of silica exposure than in those with continued silica exposure ($P < 0.05$). The sFas level was higher in non-smokers than in smokers

Table 2 The levels of AI, Fas, and caspases among silicosis patients, observers, and healthy volunteers

Group	n	AI (%)	mFas	sFas (ng/mg.pro)	Caspase-8	Caspase-3
Volunteer	13	19.6 ± 9.6	0.7883 ± 0.5232	ND	0.9058 ± 0.4532	0.5497 ± 0.1867
Observer	13	18.1 ± 1.7	0.6588 ± 0.2181	0.0450 ± 0.0312	0.8619 ± 0.0897	0.6414 ± 0.3458
Silicosis at stage I	33	31.2 ± 8.2*#	0.8707 ± 0.3748*	0.0223 ± 0.0121	0.8702 ± 0.1811	0.8585 ± 0.4579*
Silicosis at stage II + III	15	49.3 ± 13.7*#$	1.0695 ± 0.0962*#	0.0157 ± 0.0107#	0.8572 ± 0.2334	1.0164 ± 0.2202*#
χ^2/F		42.02	3.27	1.98	0.12	5.172
P		0.0000	0.0469	0.3726	0.9363	0.0753

* Compared with healthy volunteers, $P < 0.05$; # compared with observers, $P < 0.05$; $ compared with stage-I silicosis patients, $P < 0.05$. AI data was derived from FCM analysis

Table 3 The association of levels of AI, Fas, and caspases to silica exposure in silicosis patients

Indices		n	sFas (ng/ml)	mFas	Caspase-8	Caspase-3	AI (%)
Duration from silica exposure to lung lavage (year)	<20	30	0.0427 ± 0.0286	0.9170 ± 0.3570	0.9256 ± 0.1939	0.9054 ± 0.4376	34.5 ± 6.1
	20–37	18	0.0338 ± 0.0198	0.9384 ± 0.4233	0.8308 ± 0.1910*	0.9067 ± 0.3594	38.3 ± 6.9*
Duration from silica-exposure to silicosis onset (year)	<15	20	0.0370 ± 0.0298	1.0361 ± 0.4062	0.8032 ± 0.2000	1.0078 ± 0.3358	38.4 ± 7.3
	15–37	28	0.0210 ± 0.0105#	0.7914 ± 0.3509#	0.9180 ± 0.1793#	0.7478 ± 0.4656	33.9 ± 5.6#
Duration from cessation of silica exposure to lung lavage (year)	No	16	0.0339 ± 0.0223@	1.0651 ± 0.4294@	0.9060 ± 0.2450	0.9657 ± 0.3772	38.2 ± 6.6
	Yes	32	0.0488 ± 0.0214	0.8726 ± 0.3726	0.8493 ± 0.1720	0.8803 ± 0.4207	35.9 ± 6.7
Smoking	No	16	0.0410 ± 0.0261	1.0136 ± 0.4583	0.8837 ± 0.2257	1.0909 ± 0.4355	34.9 ± 6.0
	Yes	32	0.0277 ± 0.0209$	0.8903 ± 0.3635	0.8579 ± 0.1828	0.8168 ± 0.3653	37.9 ± 6.7

* Compared with duration from silica exposure to lung lavage <20 year group, $P < 0.05$; # compared with length from silica exposure to silicosis onset <15 year group, $P < 0.05$; @ compared with cessation of silica exposure, $P < 0.05$; $ compared with non-smokers, $P < 0.05$

($P < 0.05$). No significant difference in mFas, caspases, or AI was observed between smokers and non-smokers.

To adjust AM apoptosis for confounding factors including age and smoking status, the Poisson generalized linear regression model was used. AI was set as the dependent variable, and age, age at first silica exposure, duration from silica exposure to lung lavage, age of patients at the onset of pneumoconiosis, duration from silica exposure to silicosis onset, duration from cessation of silica exposure to lung lavage, silicosis type, smoking, mFas, sFas, caspase-8, and -3 were considered independent variables. As shown in Table 4, duration from silica exposure to silicosis onset, silicosis type, mFas, smoking, and caspase-8 were still associated with a role in AI after controlling for the role of confounding factors. AI increased with the level of mFas and decreased with duration from silica exposure to silicosis onset, silicosis type, and caspase-8 level. Smoking was a major confounding factor in inducing apoptosis.

Discussion

Occupational silicosis remains an urgent social and public health issue. At present, approximately 20 million workers are exposed to occupational dust. Although scientists and government have made great efforts to control dust environments, 10,000–20,000 pneumoconiosis patients are diagnosed each year in China. Understanding the mechanism of silicosis for prevention or early diagnosis remains a challenge in the field.

Epidemiologic investigation has confirmed that silicosis is directly associated with dust nature, concentration, dispersity, free silica content, and duration of silica exposure. Workers can develop acute and accelerated silicosis within a short time in workplaces with high dust concentrations, dispersity, and free silica content. Length of silica exposure directly reflects the cumulative silica burden and possibility of developing silicosis [8]. However, little is known concerning the crucial cellular and molecular mechanisms that initiate and promote the process of silicosis.

Current evidence suggests that AMs play a critical role in the development of lung inflammation and fibrosis. AMs isolated from lung fibrosis patients are activated, release a variety of fibrogenic factors and cytokines, and recruit neutrophils to alveolar space to induce alveolitis. Meanwhile, silica binding to scavenger receptors on the surface of AMs can upregulate the expression of FasL, which may in turn lead to AM apoptosis via interaction with Fas [4, 9, 10]. The protein Fas is a widely expressed member of a family of death receptors known to be involved in various forms of physiological and pathological cell death [11, 12]. Activation of the Fas receptor by Fas ligand triggers a complex cascade of intracellular events leading to caspase-8 activation and apoptosis [13, 14]. Fas-mediated apoptosis is an essential mechanism for the maintenance of normal tissue homeostasis, and disruption of this death pathway has been associated with several human diseases including lung fibrosis. Rodent experiments have suggested that the Fas/FasL pathway plays an essential role in silica-induced lung fibrosis [15, 16], but little is known concerning its role in human silicosis.

In the present study, most of the AMs from observers or silicosis patients were damaged (Fig. 1A–C) and contained dust (Figs. 1B, 2C). The apoptotic AMs of silicosis patients mainly demonstrated new crescent body formation (Fig. 1A–C), and the extent of apoptosis was related to progression of silicosis (Figs. 1A, B, 2C). AM DNA damage occurred in silicosis patients but not healthy volunteers (Fig. 2A, C). Our study revealed that the AM AI of silicosis patients was higher than those of observers and healthy volunteers, and the AI increased with the progression of silicosis (Table 2). Our results also demonstrated that longer duration from silica exposure to lung

Table 4 Analysis of the factors influencing apoptosis index

Factors	$\widehat{\beta}$	$S_{\bar{x}}$	z	*P*	95%CI
Duration from silica exposure to silicosis onset	−0.4876	0.1352	−3.60	0.000	−0.7527 to −0.2225
Pattren of silicosis	−6.8169	1.9795	−3.44	0.001	−10.6969 to −2.9370
mFas	4.4930	1.7178	2.62	0.009	1.1260 to 7.8600
Smoking	6.1636	2.5460	2.42	0.015	1.1734 to 11.1537
Caspase-8	−8.2292	3.6721	−2.24	0.025	−15.4266 to −1.0318
sFas	−1.5135	0.7682	−1.08	0.278	−2.0193 to 0.0077
Age at first silica exposure	−0.2359	0.2402	−0.98	0.326	−0.7068 to 0.2350
Caspase-3	0.5607	1.9565	0.29	0.774	−3.2739 to 4.3955

$\widehat{\beta}$ means partial regression coefficient, $S_{\bar{x}}$ means standard error of partial regression coefficient, *Z* means Non-normality test of partial regression coefficient, *P* means the significant level of Z, *95%CI* means 95% confidence interval of partial regression

lavage and shorter duration from silica exposure to silicosis onset were associated with increased AM apoptosis (Table 3). The regulation of AM apoptosis is supported by silicosis epidemiology results [8, 17] indicating that AM apoptosis is an important mechanism of silicosis. Therefore, investigation of the mechanism of AM apoptosis may provide new biomarkers for detecting and predicting early-stage silicosis in dust-exposed workers. These findings also highlight a new research direction in silicosis prevention and control. For example, screening for AM apoptosis may be used as a standard indicator for the appropriately timed cessation of silica exposure, which is an effective method to protect workers from the harm of silica particles.

Otsuki et al. [18] found that serum sFas levels were significantly higher in silicosis patients than in healthy volunteers. Domagala-Kulawik et al. [19] also reported higher Fas expression in AMs from the bronchoalveolar lavage fluid of patients with sarcoidosis. The present study demonstrated a relationship between Fas and silicosis (Table 2), including the elevation of mFas levels with the progression of silicosis (Fig. 2B). These findings indicate that exposure to silica can upregulate mFas expression in humans, which interacts with FasL resulting in procaspase-8 activation. Caspase-8 can in turn activate caspase-3, leading to AM apoptosis. These findings are partly consistent with the data reported by Otsuki et al. [18]. The expression of Fas signaling proteins directly reflects a possible mechanism of silica-induced AM apoptosis.

Our results suggest that AI, Caspase-3 and mFas levels correlate better with duration of exposure to silica and development and progression of silicosis. (Table 2, 3) The levels decreased with cessation of exposure but remained high with the development of silicosis. The decrease in level of sFas correlates better with duration of exposure however it is not significantly affected by development of silicosis. The level returned to normal after cessation of exposure.

The level of Caspase-8 increased with duration of exposure to silica but tended to decrease with development of silicosis and remain low after cessation of exposure. It is possible that with initial exposure to silica dust, the Caspase-8 level increased due to increased in demand by Caspase-3 mechanism in cells due to increased apoptosis. However, with the onset of silicosis the demand of Caspase-8 in cell may increase exponentially which the Caspase-8 mechanism is not able to meet and thus level of Caspase-8 starts to decrease though the Caspase-3 level still remained higher than normal. Therefore we suggest that Caspase-8 level may be a better indicator of the development of silicosis while a decrease in sFas is better indicator of exposure to silica. However, the apoptotic index remained good indicator of development and progressions of silicosis and may be clinically useful in determining progression of silicosis.

Tobacco smoke has been implicated as a major risk factor in pulmonary diseases. The toxicity of smoke is due to a large variety of compounds, including nicotine, cadmium, benzo[*a*]pyrene, oxidants, and free radicals, that initiate, promote, or amplify oxidative damage, which can lead to cell apoptosis and necrosis [20, 21]. In consideration of the confounding role of smoke in silica-induced AM apoptosis, the silicosis patients in this study were divided into 2 groups according to smoking or non-smoking status. No difference in AI was observed between the 2 groups, but a role for smoking in AM apoptosis appeared when the linear regression model was used. This finding indicates that silica exposure and smoking can enhance the damage to AMs and promote the development of silicosis.

To identify factors that influence AM apoptosis, multiple factor analysis was conducted in this study. The main factors affecting apoptosis were duration from silica exposure to silicosis onset, silicosis type, mFas, caspase-8, and smoking (Table 4). This result suggests that AM apoptosis and the Fas/FasL pathway may be involved in human silicosis. This type of detailed information regarding silicosis, especially the early events of pathology, in humans is very important, as it may provide indicators to predict the potential for silica-induced lung fibrosis.

In conclusion, we have shown that AM apoptosis is closely associated with the progression of human silicosis. The degree of apoptosis was related to silica exposure history, and the mechanism of silica-induced AM apoptosis was related to Fas signaling pathway activation. The results of this study may have important implications in the understanding of silicosis pathogenesis and provide a potential strategy for silicosis treatment.

Acknowledgment We would like to acknowledge the other staff from the Department of Pneumoconiosis of "Beidaihe Sanatorium for China Coal Miners" for whole-lung lavage, and also appreciate those who assisted us at Hebei United University and China Medical University. We also would like to give thanks to BioMed Proofreading, LLC for their careful copy editing. The programs were supported by the Natural Science Foundation of China (30671741), Pneumoconiosis Treatment Foundation for China Coal Miners (2005-03), and Science and Technology Support Program of Hebei Province (09276196D).

Disclaimer The findings and conclusions in this report are those of the authors and do not necessarily represent the views of the National Institute for Occupational Safety and Health.

References

1. Langley RJ, Mishra NC, Peña-Philippides JC, Hutt JA, Sopori ML (2010) Granuloma formation induced by low-dose chronic silica inhalation is associated with an anti-apoptotic response in Lewis rats. J Toxicol Environ Health A 73:669–683
2. Wang L, Scabilloni JF, Antonini JM, Rojanasakul Y, Castranova V, Mercer RR (2006) Induction of secondary apoptosis,

inflammation and lung fibrosis after intratracheal instillation of apoptotic cells in rats. Am J Physiol Lung Cell Mol Physiol 290:L695–L702
3. Davis GS (1986) Pathogenesis of silicosis: current concepts and hypothesis. Lung 164:139–154
4. Hamilton RF Jr, Thakur SA, Holian A (2008) Silica binding and toxicity in alveolar macrophages. Free Radic Biol Med 44:1246–1258
5. Tumane RG, Pingle SK, Jawade AA, Nath NN (2010) An overview of caspase: apoptotic protein for silicosis. Indian J Occup Environ Med 14:31–38
6. Aravindakshan TV, Nainar AM, Nachimuthu K (1997) High salt method: a simple and rapid procedure for isolation of genomic DNA from buffalo (Bubalus bubalis) white blood cells. Indian J Exp Biol 35(8):903–905
7. http://www.millipore.com/immunodetection/id3/westernblotting protocols#protocol
8. Liu H, Tang Z, Yang Y, Weng D, Sun G, Duan Z et al (2009) Identification and classification of high risk groups for coal workers' silicosis using an artificial neural network based on occupational histories: a retrospective cohort study. BMC Public Health 9:366–373
9. Attik G, Brown R, Jackson P, Creutzenberg O, Aboukhamis I, Rihn BH (2008) Internalization, cytotoxicity, apoptosis, and tumor necrosis factor-alpha expression in rat alveolar macrophages exposed to various dusts occurring in the ceramics industry. Inhal Toxicol 20:1101–1112
10. Hu S, Zhao H, Al-Humadi NH, Yin XJ, Ma JK (2006) Silica-induced apoptosis in alveolar macrophages: evidence of in vivo thiol depletion and the activation of mitochondrial pathway. J Toxicol Environ Health A 69:1261–1284
11. Nagata S, Golstein P (1995) The Fas death factor. Science 267:1449–1456
12. Nagata S (1997) Apoptosis by death factor. Cell 88:355–365
13. Lenardo M, Chan KM, Hornung F, McFarland H, Siegel R, Wang J et al (1999) Mature T lymphocyte apoptosis: immune regulation in a dynamic and unpredictable antigenic environment. Annu Rev Immunol 17:221–253
14. Nagata S (1999) Fas ligand-induced apoptosis. Annu Rev Genet 33:29–55
15. Borges VM, Lopes MF, Falcão H, Leite-Júnior JH, Rocco PR, Davidson WF et al (2002) Apoptosis underlies immunopathogenic mechanisms in acute silicosis. Am J Respir Cell Mol Biol 27:78–84
16. Rimal B, Greenberg AK, Rom WN (2005) Basic pathogenetic mechanisms in silicosis: current understanding. Curr Opin Pulm Med 11:169–173
17. Zhang M, Zheng YD, Du XY, Lu Y, Li WJ, Qi C et al (2010) Silicosis in automobile foundry workers: a 29-year cohort study. Biomed Environ Sci 23:121–129
18. Otsuki T, Miura Y, Nishimura Y, Hyodoh F, Takata A, Kusaka M et al (2006) Alterations of Fas and Fas-related molecules in patients with silicosis. Exp Biol Med (Maywood) 231:522–533
19. Domagała-Kulawik J, Droszcz P, Kraszewska I, Chazan R (2000) Expression of Fas antigen in the cells from bronchoalveolar lavage fluid (BALF). Folia Histochem Cytobiol 38:185–188
20. Banerjee S, Maity P, Mukherjee S, Sil AK, Panda K, Chattopadhyay D et al (2007) Black tea prevents cigarette smoke-induced apoptosis and lung damage. J Inflamm 4:3
21. D'Agostini F, Balansky RM, Izzotti A, Lubet RA, Kelloff GJ, De Flora S (2001) Modulation of apoptosis by cigarette smoke and cancer chemopreventive agents in the respiratory tract of rats. Carcinogenesis 22:375–380